CREEP PROPERTIES OF DISSIMILAR WELD JOINT OF STEELS COST FB2 AND COST F

KASL Josef, JANDOVÁ Dagmar, CHVOSTOVÁ Eva

Research and Testing Institute Plzeň, Ltd., Pilsen, Czech Republic, EU
kasl@vzuplzen.cz, jandova@vzuplzen.cz, chvostova@vzuplzen.cz

Abstract

Creep test to the rupture of the dissimilar weld joint made of COST FB2 and COST F martensitic steels was carried out at temperatures ranging from 550°C to 650°C in the stress range from 70 to 220 MPa. Creep rupture strength was evaluated using Larson-Miller parameter. Assessment of microstructure, changes of precipitates and dislocation substructure were correlated with the creep strength. Critical zones of creep damage were determined. At lower temperatures and higher stresses the weld joint ruptured in the base material of COST F steel unaffected by welding, while at higher temperatures and lower stresses rupture occurred in the intercritical heated and fine-grained parts of heat affected zone (HAZ) of steel COST F. The processes of recovery in connection with precipitation of new particles of Laves phase and their coarsening is the main causes of decrease in creep rupture strength in the HAZ of steel COST F.

Keywords: Martensitic steels, welding, creep testing, microstructure

1. INTRODUCTION

The continuous trend towards more economic electricity production together with reduced environmental pollution can be sustained by improving the thermal efficiency of power generation plants. One way to increase the efficiency of fossil power plants is to increase the temperature and pressure of the steam which finally results in the need for improved materials for the boiler and turbine design. The class of the 9-12% Cr steels is currently used for critical components in plants operating at ultra-supercritical conditions of steam. These steels show high long-term creep strength and oxidation resistance in steam, along with ease of welding and fabrication of large forgings, castings and pipe sections. The European activities in the research, development and qualification of advanced high Cr-steels were concentrated in the COST programmes. The standard material in manufacturing turbine rotors is F (10%CrMoVNbN). The trend to even higher steam conditions led to development of new promising steel FB2 [1-3].

This paper deals with the study of rupture properties and microstructure evaluation in the samples of trial dissimilar weld joint of rings made of steels COST F and COST FB2 assigned for industrial production of welded rotors.

2. EXPERIMENTS

2.1. Materials and welding process

Dissimilar weld joints were prepared from forgings of two rings (external diameter of 600 mm and thickness of 200 mm) made of steels type COST FB 2 ((X13CrMoCoVNbN9-1-1) - the base material 1 (BM 1) and COST F (X14CrMoVNbN10-1) - the base material 2 (BM 2). Producer of both the forgings was SAARSCHMIEDE Gmbh Freiformschmiede according to the specification of Doosan Skoda Power Ltd. The quality heat treatment of forgings was 1070°C/6,5h + 570°C/12,5h + 710°C/24h and 1050°C/6h + 1100°C/6h + 570/12,5h + 720/24h for the base material 1 and the base material 2 respectively. Two filler materials were tested, namely Thermanit MTS 3 (W-CrMo91) and PSM Thermanit MTS 616 (W-ZCrMoWVNb). Welds were carried out using automated welding method 141+111 (TIG HOT WIRE) into narrow gap with internal protection by argon. The thickness of welded walls was 120 mm. Three post-weld heat treatments (PWHT) processes were applied to the

weldments. On the basis of evaluation of mechanical properties, hardness and microstructure observation, the weld joint with the weld metal of THERMATIT MTS 616 and the second PWHT were chosen as the most promising variant for rotor production. For inspections of welded zones after post-heating treatments, the ultrasonic testing TOFD method was used as well as standard NDT surface inspection.

The chemical compositions of the base materials COST F and COST FB2 and the filler metal used are given in **Table 1**.

Table 1 Chemical composition in weight %

Part	Element								
	C	***Mn***	***Si***	***P***	***S***	***Cr***	***Ni***	***Mo***	***V***
Base material FB2	0.13	0.34	0.08	0.005	0.001	9.06	0.17	1.48	0.20
Weld metal MTS 616	0.11	0.42	0.30	0.005	0.003	8.87	0.57	0.56	0.18
Base material 2 F	0.11	0.56	0.06	0.008	0.002	10.36	0.64	1.46	0.20

Part	Element								
	Co	***W***	***Nb***	***N***	***B***	***Al***	***Sn***	***As***	***Sb***
Base material FB2	1.32		0.059	0.016	0.0079	0.007	0.002	0.008	< 0.001
Weld metal MTS 616	0.15	1.49	0.051	0.018	0.0036	0.009	0.003	0.022	< 0.001
Base material 2 F			0.059	0.016	0.0079	0.009			

2.2. Materials and welding process

Smooth cross-weld specimens with a length of 92 mm and a diameter of 8 mm were fabricated from the weld joint. Creep tests to the rupture of these specimens were carried out. Fracture surfaces of ruptured samples were observed using scanning electron microscope (SEM). Then specimens were cut along their longitudinal axis. Macrostructure was revealed using Villela-Bain´s reagent and location of fracture in the weldment was specified. Hardness measurement along the specimen axis was performed. Microstructure of longitudinal sections was observed using light microscopy (LM) and scanning electron microscopy (SEM). The substructure was evaluated in a transmission electron microscope (TEM).

3. RESULTS

3.1. Mechanical properties

Integrity and mechanical properties of weld joint have been evaluated according to the welding standards EN 288-2.3. All results were satisfactory.

3.2. Creep test

The creep rupture testing was carried out in air at temperatures ranging from 550°C to 650°C and stresses from 70 MPa to 220 MPa. The longest time to the rupture of samples so far is about 22,000 hours. Obtained creep data were evaluated using the Larson-Miller parametric equation:

$$P = T * [C + \log \tau], \quad (1)$$

where T represents temperature given in degree Kelvin, C is a specific constant for a given material (equal 36) and τ means time to rupture in hours. Results of creep strength of the weld joint compared with the creep rupture strength data of COST F steel [4] are graphically represented in **Fig. 1**. Open symbols indicate creep tests, which are still running.

The current creep data Samples tested at 550°C (one sample is still in progress) are in the permitted scatter band ± 20 % of the creep strength of the base material COST F. The creep strengths of all ruptured samples tested at 575°C (one sample is still in progress) are comparable with creep strength of the base material. The creep strengths of (ruptured) samples tested at 600°C are on the level of the base material COST F with the exception of the samples tested at the lowest stressesa. The creep strengths of the samples tested at 625 °C (all tested samples broken) fall into the scatter band ± 20 % of the creep strength of the base material COST F with the exception of the sample tested at the lowest stress, which is below this scatter band. The creep strengths of samples tested at the highest temperature 650°C are inside of the scatter band.

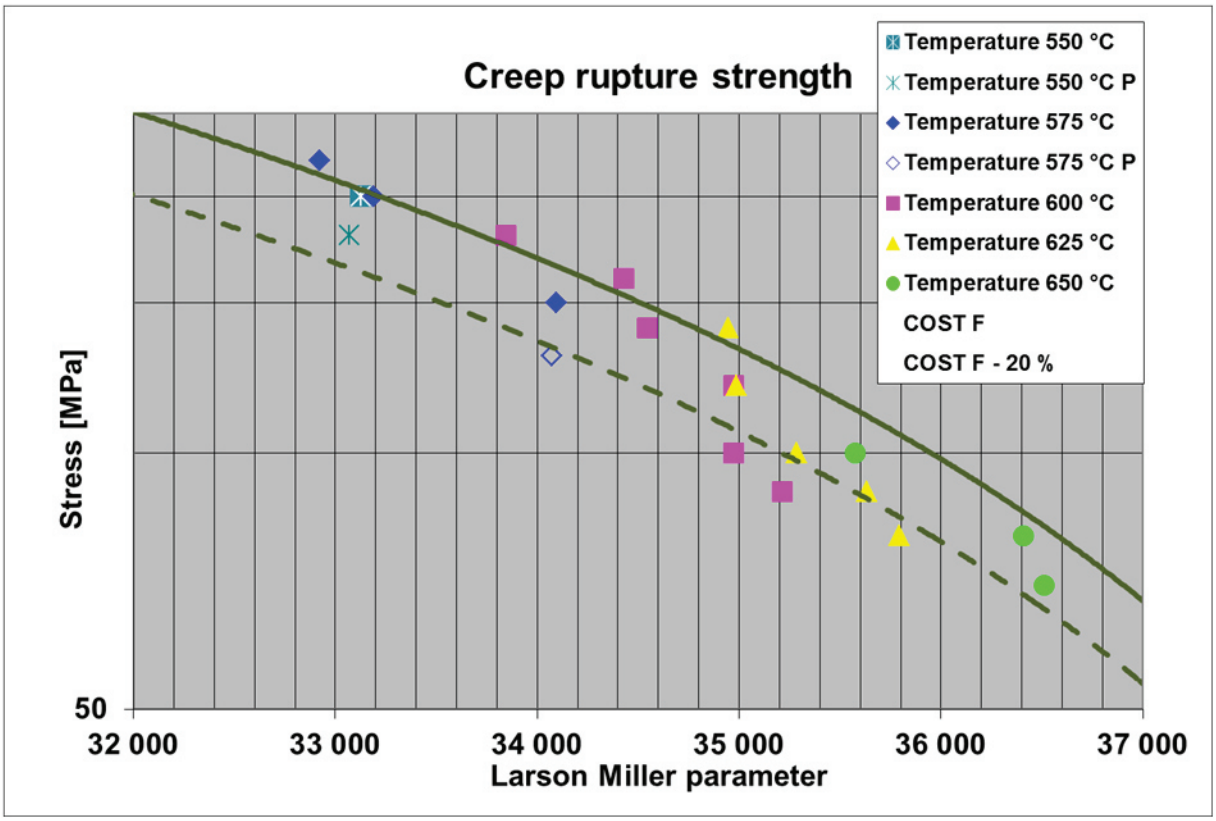

Fig. 1 Creep rupture strength vs. LMP

3.3. Fractography

Fractographic analysis of broken samples was performed. This analysis and observation of longitudinal sections of the ruptured crept samples showed that locations of fractures depended on the creep conditions. The samples tested at lower temperatures and higher stresses failed in the base material (BM) of steel COST F unaffected by welding while those tested at higher temperatures and lower stresses ruptured in the grain refined part (FG) or in the intercritically reheated part (IC) of the heat-affected zone (HAZ) of the base material of steel COST F. Ductile fracture in the BM occurred after short durations of creep tests (up to 2,700 hours). The fractures are transcrystalline ductile with considerable macroplastic deformation (elongation about 18%) and with the dimple morphology of the fracture surface. Other samples ruptured by transgranular creep fracture

in the HAZ of the steel COST F. Elongations of these specimens were usually a few percent. Individual small cracks formed of growing cavities joined and spread step by step across the sample. Exact positions of fracture change from IC part of the HAZ to boundary between FG and CG parts of the HAZ with increasing temperature and decreasing stress.

3.4. Hardness

Hardness HV10 profiles across the weld joints were determined for the weld joint before and after creep testing. Before creep testing the average hardness of both the base materials was about 240 and hardness of the WM about 280. Local minima were found in the fine grained or in the overheated part of the HAZs - 204 in the steel COST FB2 and 218 in the steel COST F.

During creep test (up to duration of about 11,000 hours) the most significant decrease of hardness occurred in the IC part of HAZ of steel COST F (**Fig. 2**). After the creep test at 625°C and 120 MPa the hardness fell to a level of about 180. A larger decrease of hardness of the base material COST F was also found - from 233 to 204 (sample tested at 625°C/120 MPa). On the other hand the hardness drop of both the base material COST FB2 and its HAZ was not so considerable. From 236 to 218 (sample 625°C/120 MPa) and from 204 to 194 (sample 625°C/90 MPa) for the base material and HAZ of COST FB2 respectively. The hardness of the weld metal only slightly decreased from 277 to 260 (sample tested at 650°C/70 MPa).

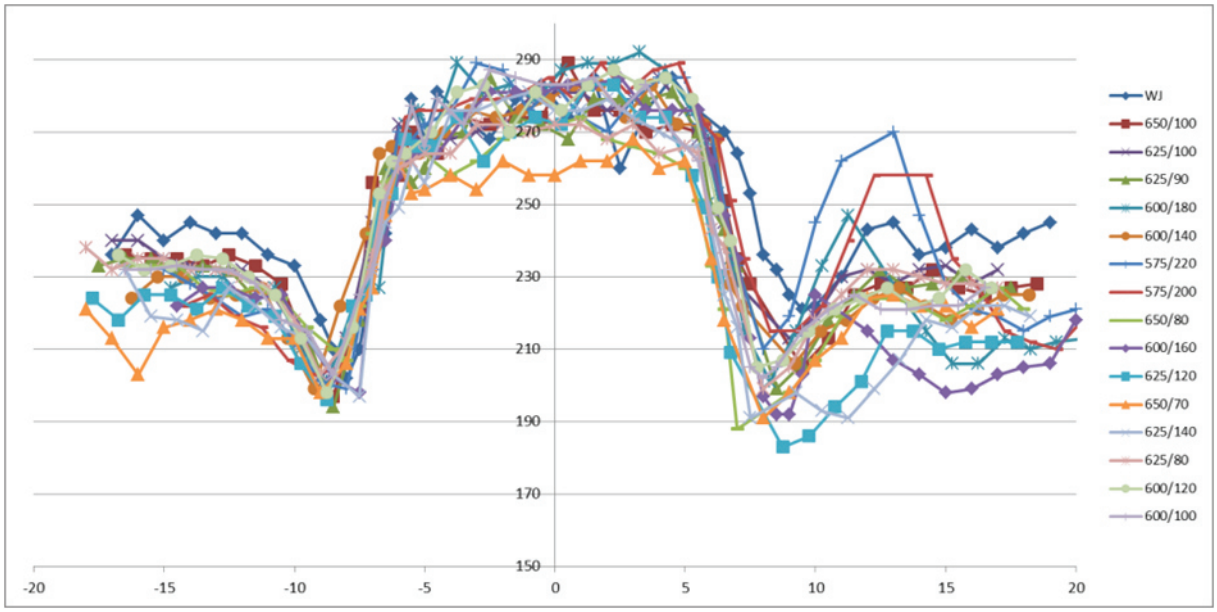

Fig. 2 Creep rupture strength vs. LMP

3.5. Structure

The width of heat affected zones ranges from 2.5 to 3.0 mm on both sides of the weldment. Usual globular aluminium oxides are present in steel COST FB2. Steel COST F contains only a few small particles of aluminium oxides containing calcium and magnesium. Aluminates together with silicon oxides are present in the weld metal. The addition of boron into the alloy stabilizes the martensitic structure (especially $M_{23}C_6$ particles and grain boundaries). However, excess in the addition of nitrogen in combination with boron causes the formation of primary boron nitrides during heat treatments with consequent decrease of the beneficial effects of boron addition. This effect occurred in steel COST FB2, which contains a relatively large number of particles of BN with a size of several micrometres. They are often joined with coarser niobium carbides.

Sizes of prior-austenitic grains are different in various parts of the weldment. Grain size of steel COST FB2 (about 90 μm) is significantly larger in comparison with steel F (about 21 μm). Average grain sizes of both the

HAZs and the weld metal are comparable with grain sizes of steel F (about 20 μm). Grain sizes of coarse-grained parts of HAZs are only slightly larger compared with fine-grained parts of HAZs; from 28 to 17 μm and from 38 to 14 μm for HAZ FB2 and HAZ F respectively. Also average grain sizes in both the cast and heated parts of the weld metal are similar although the form of the grains is different.

Microstructure of the base materials in FB2 consisted of heavy tempered martensite with a small amount of δ-ferrite. Coarser prior austenitic grains contain packets of martensitic laths. Transmission electron microscopy of carbon replicas and thin foils showed that some of them are subdivided into subgrains. The main contributor in suppressing the recovery of martensitic structure was a dispersion of $M_{23}C_6$ and fine vanadium carbonitride particles. However non-uniform distribution of fine vanadium carbonitrides was observed within laths. Dislocation density was about $4 \cdot 10^{14}$ m^{-2}.

The weld metal also consisted of tempered martensite containing islands of δ-ferrite. Structural changes in relation to position - cast structure with elongated grains in individual beads and more polygonal shape of grains inside the heat affected zones of the upper weld passes. Coarser particles of carbides rich in W, Mo, Cr, V together with some rare particles of Laves phase were observed in the WM, which is alloyed with tungsten. Some ferritic laths were subdivided into subgrains. Dislocation density was about $5 \cdot 10^{14}$ m^{-2}. The main precipitate was $M_{23}C_6$, fine particles of V(N,C) were also present.

The base metal F is fine-grained. Similar average grain size was also observed in the HAZ with only slightly higher average size in coarse-grained region. Martensitic lath structure is conserved here and laths contain subgrains only locally (**Fig. 3a, b**). On the other hand prior austenitic grains are subdivided into small equiaxed subgrains or new grains in the fine-grained region. Fine vanadium/niobium MX carbonitrides were spread within ferrite laths more often in steel F and also in the weld metal than in steel COST FB2. In contrast, the density of chromium carbides was higher in steel COST FB2 than in other parts of the weldment. Dislocation density in steel F was the highest, about $6 \cdot 10^{14}$ m^{-2}.

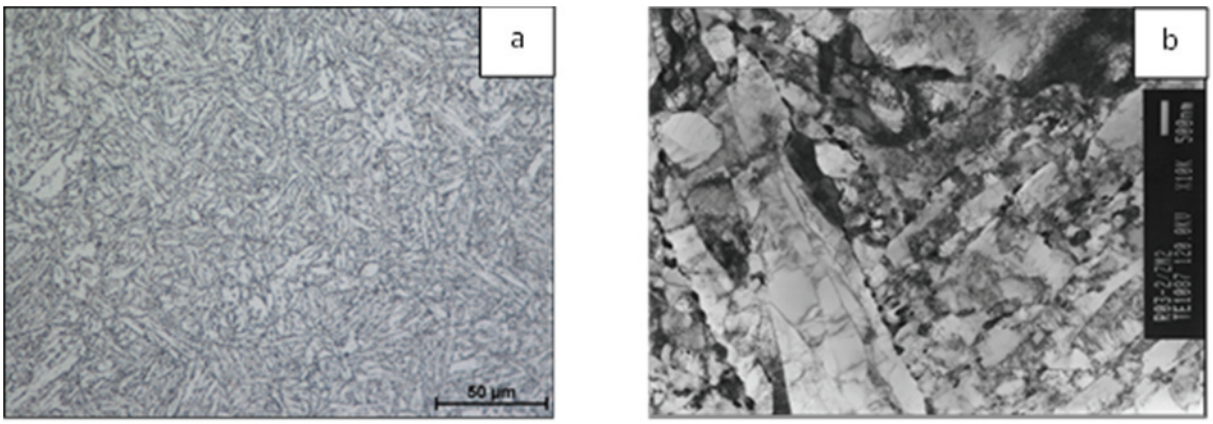

Fig. 3 Microstructure of the base material F - LM (a) and TEM (b)

No significant changes after creep testing were observed after a short test time of several hundred hours. However, a relatively massive precipitation of particles of Laves phase occurred after a relatively short duration of creep (about 2,000 hours) especially in the HAZ of steel F. Comparison of the formation of new particles of Laves phase during creep testing inside the HAZ of the steel COST FB2 is shown in SEM-micrographs in **Fig. 4** (these particles are visible as bright objects in back-scattered electrons figures). Similar states were observed in both the base materials and the weld metal. However precipitation of Laves phase particles was retarded in steel COST FB2.

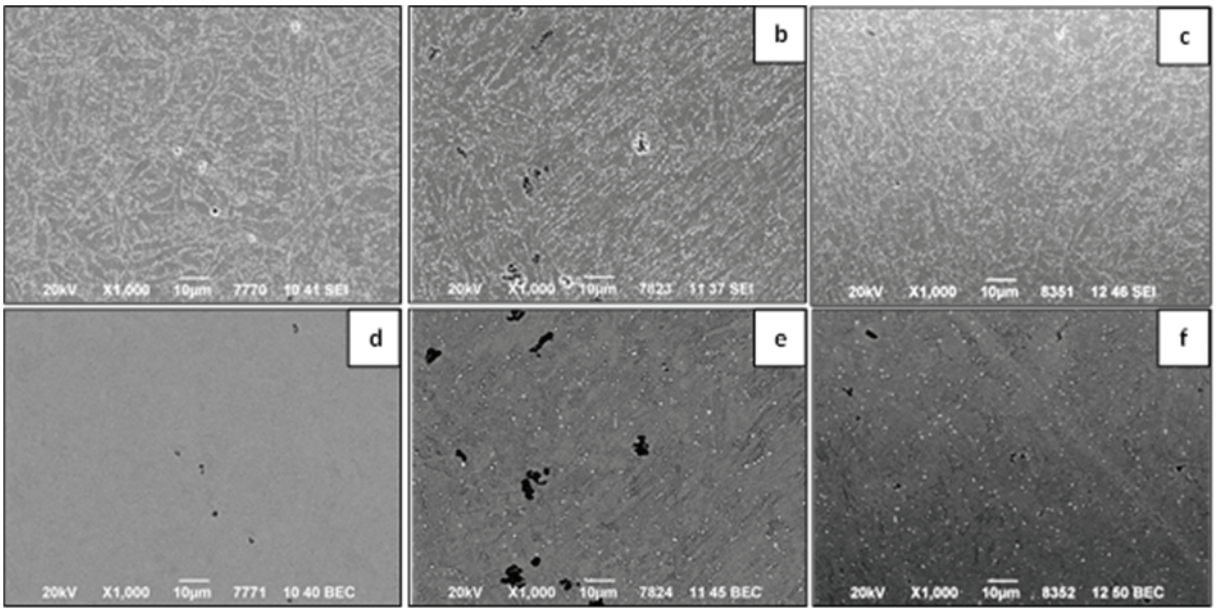

Fig. 4 Precipitation of particles of Laves phase in the FG HAZ of the base material F - SEM, secondary (a-c) and backscattered electrons image (d-f); after PWHT (a,d), 625 °C/80 MPa, 7,137 hours (b,e) and 600 °C/100 MPa, 11,288 hours (c,f)

Many cavities were indicated in the HAZ of steel COST F after creep test with duration of more than 2,000 hours. They are concentrated inside the fine-grained and over-tempered parts. Microstructure in the HAZ of steel F exhibited a subgrain/grain structure often of polygonal shape instead of typical martensitic lath-like structure (**Fig. 5**). Interiors of grains are free of particles of precipitates. This region represents a weak link in the system.

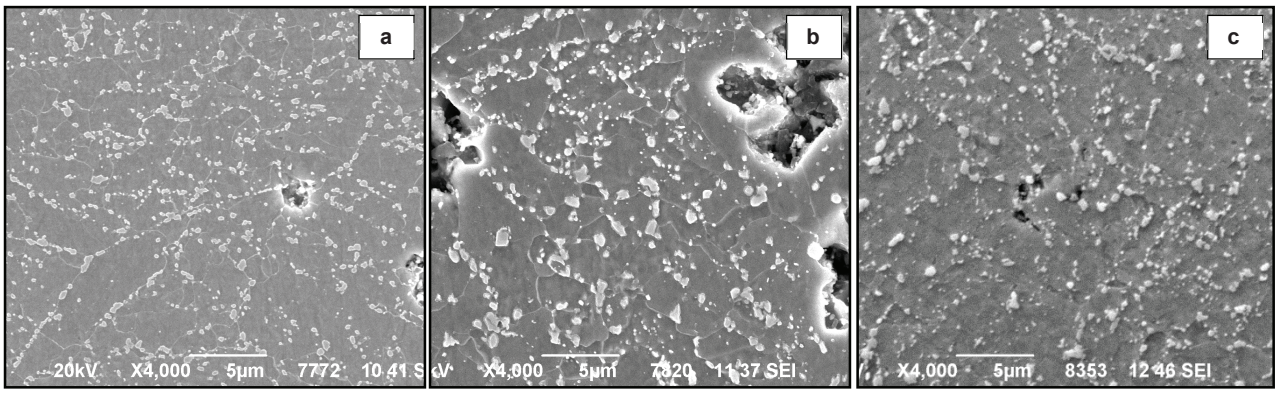

Fig. 5 Microstructure of the CG HAZ (b) of the base material F - SEM; after PWHT (a), 625 °C/80 MPa, 7,137 hours (b) and 600 °C/100 MPa, 11,288 hours (c)

4. CONCLUSIONS

From the results gained so far the following conclusions can be made:

Creep strength of the examined weld joint falls into ±20% scatter band of the creep strength of the corresponding base material COST F up to 600°C. For testing temperature 625°C the creep strength of the weld joint decreases below the scatter band for samples tested at low stresses. However, for testing temperature 650 °C it is inside the scatter band.

After post-weld heat treatment the hardness of the weld metal is 280 HV10; local minima are at a comparable level in the fine-grained parts of the HAZ in both the base materials. During creep testing the highest decrease of the hardness occurred in the intercritically reheated or in the over-tempered parts of HAZ of steel F where samples failed.

The samples tested at lower temperatures and higher stresses failed in the base material of steel COST F while those tested at higher temperatures and lower stresses ruptured in the grain refined part or in the intercritically reheated part of the heat-affected zone of the base material of steel COST F.

After a relatively short time (about 2,000 hours) precipitation of Laves phase occurred in all parts of the weld joint. It is significant in the HAZ of steel F, where coarsening of M23C6 occurred. With increasing time to rupture both coarsening and new precipitation of particles of Laves phase and cavitation formation occurred. Cavities were originated in the intercritically reheated or in the over-heated parts of HAZs of steel F where fine grain/subgrain structure is formed due to the recovery.

ACKNOWLEDGEMENTS

This work was supported by Grant TE01020068 from the Technology Agency of the Czech Republic.

REFERENCES

[1] BERGER C., SCARLIN R.B., MAYER K.H., THORNTHON D.V., BEECH S.M.: Steam turbine materials: High Temperature Forgings. In: Proc. COST Conference on High Temperature Materials for Power Engineering, October 3-6, 1994, Liege, Belgium.

[2] KERN T.U., STAUBLI M., MAYER K.H., ESCHER K., ZEILER G.: The European Effort in Development of new High Temperature Rotor Materials up to 650°C - COST 522. In: Proc. 7th Liege COST Conference, September 29 - October 2, 2002, Liege, Belgium.

[3] KERN T.U., STAUBLI M., MAYER K.H., DONTH B., ZEILER G.: The European Effort in Development of new High Temperature Rotor Materials - COST 536. In: Proc. 8th Liege COST Conference, September 19 - 20, 2006, Liege, Belgium.

[4] Results of creep test COST 522 programme.